

1 Giant meandering channel systems controlled by sediment supply 2 to the deep-water Campos basin

3 **Jacob A. Covault, Zoltán Sylvester, Daniel T. Carruthers, and Dallas B. Dunlap**

4 *Bureau of Economic Geology, Jackson School of Geosciences, University of Texas at Austin,*
5 *Austin, TX 78713*

7 **ABSTRACT**

8 Large meandering submarine-channel systems are important conduits for mass transfer to
9 continental margins; wider and deeper channels, with larger meanders, reflect larger sediment
10 discharge. Some large meandering channel systems are known to receive voluminous sediment
11 from the largest rivers in the world, such as the Ganges-Brahmaputra, Amazon, Indus, Mississippi,
12 and Zaire (Congo); however, smaller rivers draining rapidly uplifting landscapes can also
13 contribute significant terrigenous mass to continental margins. Here, we use three-dimensional
14 seismic-reflection data from >2 km water depth in the Campos basin, offshore Brazil, to interpret
15 the stratigraphy of a Late Cretaceous submarine-channel system within a deep-water salt-tectonic
16 province. We mapped three regional seismic-reflection horizons, which define a sequence of at
17 least 16 downstream-translating channel elements ~1 to >1.5 km wide with wavelengths ranging
18 from 8 to 24 km. These are among the largest meandering channel forms and deposits in the world.
19 Increased sediment discharge through submarine channels during the Late Cretaceous, driven by
20 dynamic uplift along the humid and warm coast of southeastern Brazil, promoted the development
21 of these large meandering channels. Analogous settings characterized by rapid uplift of coastal
22 mountains and unstable, narrow shelves might promote large sediment supply to continental

23 margins, producing giant submarine canyon-channel-fan depositional systems and petroleum
24 reservoirs.

25

26 **INTRODUCTION**

27 Deep-water channels are conduits through which turbidity currents transport terrigenous
28 mass, including sediment and dissolved chemical loads, across continental margins to submarine
29 fans (Piper and Normark, 2001). This sediment and chemical transfer shapes the seascape of
30 continental margins, constructs a stratigraphic record of tectono-climatic environmental changes,
31 and plays an important role in biogeochemical cycles. For example, the Bengal fan receives a large
32 sediment load from rivers draining the rapidly uplifting Himalayas (~1 Bt/yr; Islam et al., 1999)
33 and, as a result, it comprises wide, deep, meandering submarine channels feeding the largest
34 accumulation of detritus on Earth (Barnes and Normark, 1985; Schwenk and Spieß, 2009; Kolla
35 et al., 2012). Other large submarine fans, such as the Amazon, Indus, Mississippi, and Zaire
36 (Congo), include meandering channels similar in shape and size to the Bengal. Based on insights
37 from rivers, the morphology of such meandering submarine channels reflects their importance in
38 mass transfer to continental margins; wider and deeper channels have larger meanders (Leopold
39 and Wolman, 1960; Pirmez and Imran, 2003; William, 1986), reflecting larger sediment discharge
40 (e.g., Leopold and Maddock, 1953; Konsoer et al., 2013).

41 Large meandering submarine-channel systems are fed voluminous sediment from some of
42 the largest rivers in the world (Summerfield and Hulton, 1994; Milliman and Farnsworth, 2011).
43 However, smaller rivers draining rapidly uplifting landscapes can also contribute significant
44 terrigenous mass to continental margins (Milliman and Syvitski, 1992). For example, high-relief,
45 tectonically active islands of the southwest Pacific Ocean, including New Zealand, Taiwan,

46 Indonesia, Malaysia, Papua New Guinea, and the Philippines, make up only ~3% of the Earth
47 landmass, but the short lengths and steep gradients of the rivers and the high variability of rainfall
48 promote large fluvial sediment loads (collectively ~7 Bt/yr suspended sediment; Milliman and
49 Farnsworth, 2011) to be routed from mountains to the ocean (Milliman and Syvitski, 1992). So,
50 although some of the largest meandering submarine-channel systems in the world are linked to
51 large rivers, we also expect similarly large submarine channels on the present seafloor and in
52 ancient sedimentary successions linked to rivers draining small, tectonically active catchments
53 (Milliman and Syvitski, 1992).

54 Here, we use three-dimensional (3D) seismic-reflection data from the deep-water Campos
55 salt basin, offshore Brazil, to interpret the stratigraphic evolution of a giant Late Cretaceous
56 submarine-channel system (Fig. 1). During the Late Cretaceous (Campanian-Maastrichtian), small
57 rivers draining humid and warm, tectonically active coastal mountains of southeast Brazil provided
58 voluminous sediment to the Campos-basin margin, which is characterized by rapid progradation
59 (Bruhn and Walker, 1995; Milani et al., 2007; Fetter et al., 2009; Macgregor, 2013). These tectono-
60 climatic conditions provide an opportunity to evaluate the hypothesis that small coastal rivers with
61 appreciable sediment discharge can promote the development of giant meandering submarine-
62 channel systems. Therefore, we will compare the Late Cretaceous timing of the documented
63 voluminous sediment delivery to the Campos basin margin to the contemporaneous stratigraphic
64 record of submarine-channel evolution in the Campos basin. We will measure the scale of
65 meandering submarine channels (width and meander wavelength) in the Campos basin for
66 comparison to some of the largest meandering channels on the present seafloor.

67

68 **GEOLOGIC SETTING**

69 The Campos basin is located along the southeastern continental margin of Brazil in the
70 South Atlantic Ocean (Fig. 1). It is one of the most productive deep-water hydrocarbon basins in
71 the world (Mohriak et al., 1990; Bruhn et al., 2003). The Campos basin initiated during Late
72 Jurassic breakup of Gondwana and opening of the South Atlantic Ocean (Guardado et al., 1989)
73 and comprises Berriasian-early Aptian continental rift deposits, overlain by middle Aptian salt
74 (Davison, 2007; Karner and Gamboa, 2007; Winters, 2007), an early-middle Albian carbonate
75 platform, and a late Albian to present succession of progressively deeper-water continental-margin
76 deposits (Bruhn, 1998). The Aptian salt plays an important role in establishing the structural style
77 of the Campos basin; deformation was initiated by early Albian eastward basin tilting and
78 subsequent gravity spreading as progradation occurred (Demercian et al., 1993; Davison et al.,
79 2012; Quirk et al., 2012; De Gasperi and Catuneanu, 2014). The Cretaceous-present paleoflow
80 direction through submarine-channel systems is generally northwest-to-southeast because of the
81 regional slope of the Brazilian continental margin. However, paleoflow direction in the Campos
82 basin varies depending on local structural configuration and diapir orientation; Covault et al.
83 (2019) interpreted north-to-south paleoflow for a Miocene channel system, and Ceyhan (2017)
84 interpreted northwest-to-southeast, west-to-east, and north-to-south paleoflow for Pliocene-
85 Pleistocene channel systems. We focused on a Late Cretaceous submarine-channel system in a
86 structural domain generally characterized by extensional and contractional salt stocks and walls
87 formed during west-to-east translation of surrounding minibasins across the margin (Demercian et
88 al., 1993; Mohriak et al., 2012).

89 During the Late Cretaceous (Campanian-Maastrichtian), the Trindade mantle plume
90 promoted dynamic uplift along the humid and warm coast of southeastern Brazil (Bruhn and
91 Walker, 1995; Thompson et al., 1998; Cobbold et al., 2001; Meisling et al., 2001; Fetter et al.,

92 2009; Quirk et al., 2013). High-relief coastal mountains were drained by small rivers, which
93 provided sediment directly to submarine canyons, which had incised across an unstable, narrow
94 shelf (Fetter et al., 2009). The Late Cretaceous Campos basin is characterized by rapid
95 progradation of the margin (Guardado et al., 2000; Milani et al., 2007; Fetter et al., 2009;
96 Macgregor, 2013) and large, coarse-grained, channelized petroleum reservoirs (e.g., Roncador
97 Field; Rangel et al., 1998). We will compare these upstream tectono-climatic events to the
98 contemporaneous evolution of a submarine-channel system in >2 km water depth of the Campos
99 basin.

100

101 **DATA AND METHODS**

102 **Subsurface data and interpretation**

103 We used a Kirchhoff pre-stack depth-migrated 3D seismic-reflection volume with
104 wavelengths of ~50-100 m (vertical resolution ~12.5-25 m) and 25 m horizontal sampling rate.
105 The seismic-reflection volume was donated by Investigaç o Petrol fera Limitada (PGS). Seismic-
106 reflection data were processed to zero phase. We used the Paradigm® SeisEarth® interpretation
107 and visualization product suite to map three regional horizons based on line-by-line continuity and
108 terminations of relatively high-amplitude seismic reflections. We used root mean square (RMS)
109 amplitude maps to highlight channel systems.

110

111 **Ages of seismic-reflection horizons**

112 We focused on a Late Cretaceous submarine-channel system between two regional
113 horizons: a basal Horizon 1 and a top Horizon 3 (Figs. 2 and 3; Supplementary Files 1 and 3). We
114 mapped an intermediate Horizon 2 to capture the evolution of the channel system and constrain

115 RMS amplitude maps (Fig. 3; Supplementary File 2). We did not have well data to calibrate the
116 seismic-reflection data; however, previous studies that overlap with our study area provide enough
117 well-to-seismic calibration to identify and approximate the age of the key seismic-reflection
118 horizons (Guardado et al., 1989; Fetter, 2009; Mohriak et al., 2009; Quirk et al., 2012). We
119 interpreted a regional Upper Cretaceous, potentially Campanian (Fig. 7 of Quirk et al., 2012),
120 horizon overlying a Santonian horizon (Fig. 15.38 of Mohriak et al., 2009). This horizon is the
121 base of our channel system of interest (Horizon 1); it is a high-amplitude peak characterized by
122 channel geometries and truncation of underlying reflections, which is described below in the
123 ‘Seismic Stratigraphy and Channel Morphology’ section. We interpreted another regional seismic
124 reflection to be approximately the top Cretaceous (see Figs. 8 and 9 of Fetter, 2009; Figs. 15.30,
125 15.38, and 15.39 of Mohriak et al., 2009; and Fig. 7 of Quirk et al., 2012). The top Cretaceous
126 regional horizon of Guardado et al. (1989), focused on the proximal part of the margin, appears to
127 correlate with these interpretations. This horizon is the top of our channel system (Horizon 3); it
128 is a variable-amplitude peak that appears to be truncated by high-amplitude, channelized seismic
129 reflections of Paleogene age. To the south and east of our study area, the top Cretaceous horizon
130 separates more continuous, low- to moderate-amplitude reflections from an overlying interval of
131 lower-amplitude, faulted reflections.

132

133 **How do we measure the size of a submarine channel?**

134 A common measure of a river channel is the bankfull discharge (Leopold and Wolman,
135 1960); channel shape and dimensions of meandering rivers are associated with bankfull flow
136 (Wolman and Miller, 1960). As turbidity currents do not have a well-defined upper boundary, it is
137 less obvious what can be considered as bankfull. On the seafloor, channel systems of large

138 submarine fans commonly comprise erosional valleys oriented parallel to the steepest descent
139 downstream, with a relatively narrow, sinuous channel form in the deepest location in the valley
140 (i.e., the thalweg) (Fig. 4A). The depths of submarine-channel systems from thalweg to levee crest
141 can be as many as 10-100 times larger than bankfull depth in rivers, and levee-crest widths can be
142 2-3 times wider than rivers (Pirmez and Imran, 2003; Konsoer et al., 2013; Shumaker et al., 2018).
143 However, the planform characteristics of submarine channels and rivers are remarkably similar
144 (e.g., Flood and Damuth, 1987). This suggests that the effective width and depth of turbidity
145 currents that form submarine channels and determine the nature and dimensions of the planform
146 are often narrower and shallower than the outer-levee-crest widths and levee-thalweg depths
147 (Pirmez and Imran, 2003). Both the velocity and concentration maxima of turbidity currents occur
148 near the base of the flow (Sequeiros et al., 2010; Eggenhuisen and McCaffrey, 2012). This high-
149 velocity core is likely to be thinner and narrower than the full channel or canyon form, and it is the
150 portion of the flow that contains most of the sediment load (Luchi et al., 2018) and actively sculpts
151 the meandering planform of the channel (Pirmez and Imran, 2003). In the Zaire (Congo) Canyon,
152 the largest observed turbidity currents were largely restricted to the bottom 40 m, a depth that
153 corresponds to the part of the canyon that seems to have a characteristic width (Azpiroz-Zabala et
154 al., 2017). These characteristic channel forms are often recognizable in the subsurface seismic-
155 reflection data as well, especially when they are abandoned and passively filled, and therefore well
156 preserved. The most recent channel on the proximal Bengal fan has a well-defined meandering
157 planform with a characteristic width that is much smaller than the distance between the outer-levee
158 crests (Fig. 4A). The latter is a measure of the channel-belt width, and has no direct relation to the
159 characteristic discharge of the channel-shaping flows. Similar morphologies develop in forward
160 models of submarine channel-levee systems (Figs. 4B and 4C; Sylvester et al., 2011; Sylvester and

161 Covault, 2016; Covault et al., 2016). The deposits within the narrow, sinuous channel form located
162 at the bottom of the system have been called ‘channel elements’ (Mutti and Normark, 1987; Fildani
163 et al., 2013; Hubbard et al., 2014), which have been interpreted to migrate and stack over time to
164 produce larger-scale, composite channel systems (e.g., Deptuck et al., 2003; Mayall et al., 2006;
165 Hodgson et al., 2011; McHargue et al., 2011; Sylvester et al., 2011; Covault et al., 2016; Fig. 4C).

166 We measured channel widths and meander half wavelengths that correspond to this
167 characteristic channel form. Meander wavelengths were estimated through the automatic
168 identification of inflection points along the channel centerline (see Sylvester et al., 2013; and
169 Sylvester and Pirmez, 2017; for details). We used this approach on maps of submarine channels
170 of the Bengal fan (Kolla et al., 2012), offshore West Africa (the Dalia channel system; Abreu et
171 al., 2003), and the Gulf of Mexico (Joshua Channel; Posamentier, 2003; Kramer et al., 2016). We
172 replotted data collected by Pirmez (1994) for the Amazon channel. We have also plotted width-
173 wavelength data for rivers (Leopold and Wolman, 1960; Howard and Hemberger, 1991) and
174 unpublished data from the Purus river in Brazil that was collected using the mapping techniques
175 described in Sylvester et al. (2019).

176

177 **SEISMIC STRATIGRAPHY AND CHANNEL MORPHOLOGY**

178 We mapped three Late Cretaceous seismic-reflection horizons, 1-3, from base to top,
179 within a paleotopographic low surrounded by salt diapirs (Figs. 2 and 3; Supplementary Files 1-
180 3). Horizon 1 (Upper Cretaceous, potentially Campanian) is defined by the bases of numerous
181 high-amplitude, discontinuous, channel-form seismic reflections. In Figure 3A, the western
182 margins of these channel-form reflections are commonly preserved, with the eastern margins
183 eroded, and they predominantly stack from west to east. Some of the margins of the channel forms

184 appear to transition into lower-amplitude, continuous seismic reflections. We interpret the high-
185 amplitude, discontinuous reflections to be coarse-grained channelized deposits and the lower
186 amplitude, continuous seismic reflections to be finer-grained levee-overbank deposits based on
187 seismic-facies models of deep-water depositional systems (Normark et al., 1993; Abreu et al.,
188 2003; Deptuck et al., 2003). In Figure 3A, channel forms appear to climb and vertically stack up
189 to horizon 2, which is an intermediate, regionally mappable horizon defined by channel forms
190 transitioning into lower-amplitude, continuous reflections. In the central part of the study area,
191 horizon 2 appears to truncate low-amplitude, continuous reflections; in the east, horizon 2 appears
192 to truncate high-amplitude channel-form reflections. Horizon 3 (top Cretaceous) is the top of the
193 seismic sequence and it appears to truncate underlying seismic reflections (Fig. 3).

194 Figures 5A-D show ~16 high-RMS-amplitude, sinuous ribbons between horizons 1 and 3,
195 which correspond with the high-amplitude channel forms in cross sections of Figure 3. We
196 interpret these channel-form ribbons to record the downstream translation of a large submarine-
197 channel system. Although the channel system appears to comprise as many as 16 individual
198 ‘channel elements’ *sensu* Fildani et al. (2013), we are most confident in segments of the channel
199 geometries mapped on horizons 1-3 (Supplementary Files 1-3), which indicate widths between ~1
200 to >1.5 km and half wavelengths ranging from ~4-12 km (Fig. 6, lower right, inset). Each of these
201 channel elements appears to meander and, in aggregate, they are stacked to produce the channel
202 system between horizons 1 and 3. Horizon 1 is the base of this large meandering channel system;
203 horizon 2 is an intermediate horizon deposited after one of the smaller meander loops in the central-
204 eastern part of the study area was cut off; horizon 3 is the top of this channel system, which was
205 eroded by a younger channel system (Fig. 3).

206

207 **DISCUSSION: GIANT MEANDERING SUBMARINE CHANNEL SYSTEMS**

208 Figure 6 shows a plot of widths and meander wavelengths of some of the largest
209 meandering channels on the seafloor and channel elements of the lower Miocene Dalia channel
210 system, a hydrocarbon reservoir in the subsurface offshore West Africa (Abreu et al., 2003). Some
211 of the largest rivers in the world deliver sediment to the seafloor channels, which, in turn, disperse
212 it across some of the largest submarine fans in the world, including the Amazon and Bengal. The
213 Dalia system received sediment from West Africa but prior to the Pliocene onset of the modern
214 Zaire (Congo) river and submarine canyon-fan system (Ferry et al., 2005). The seafloor channels
215 of the largest submarine fans in the world far exceed the size of the Dalia channel elements, which
216 are similar in size to other subsurface channel systems in West Africa (e.g., McHargue et al., 2011).
217 However, the Late Cretaceous channel elements in the Campos basin are wider and their meanders
218 are larger than the Amazon and Bengal submarine channels and some of the largest river bends on
219 Earth.

220 Although no discharge measurements are available for these systems, the channel widths
221 we have measured are likely linked to the characteristic discharge of the channel-forming turbidity
222 currents, just like fluvial channel dimensions are related to river discharge (Leopold and Maddock,
223 1953; Konsoer et al., 2013). The unusually large channel widths and meander wavelengths
224 observed in the Campos basin suggest that turbidity currents shaping these channels had larger
225 discharges than those responsible for building the largest submarine fans on Earth. Both the Bengal
226 and Amazon channels are ultimately fed by large rivers with large drainage areas; however, the
227 Campos basin received sediment from small, dynamically uplifting coastal rivers (Fetter et al.,
228 2009). The size of channels described here attest to the extraordinary sediment discharges of the
229 turbidity currents that shaped them. The landscape evolution modeling work of Braun et al. (2013)

230 suggests that, despite being characterized by low slopes, dynamic topography related to mantle
231 plumes can result in significant pulses of erosion and sediment flux.

232 The idea that small rivers drain rapidly uplifting landscapes and deliver voluminous
233 terrigenous sediment to continental margins is not new; this has been hypothesized since
234 researchers began to compile global sediment loads from stream gauges (e.g., Milliman and
235 Syvitski, 1992; Milliman and Farnsworth, 2011). For example, on the seafloor, offshore New
236 Zealand, the Hikurangi channel is a large (several km wide), long (~1500 km) sinuous submarine-
237 channel system receiving voluminous sediment from small rivers draining rapidly uplifting
238 mountains since the late Miocene (Lewis, 1994). In the subsurface, a large (3-5 km wide,
239 composite channel ‘belt’), sinuous submarine-channel system in the Molasse foreland basin,
240 Austria (Upper Puchkirchen Formation; De Ruig and Hubbard, 2006), developed in response to
241 an increase in early Miocene sediment supply from the tectonically active Alps (Kuhlemann, 2007;
242 Sharman et al., 2018). However, it is challenging to decipher the evolution of meanders in these
243 systems and other examples; seafloor examples represent static images of a moment in time, and
244 some subsurface studies primarily characterize the composite channel-belt fill rather than the
245 smaller-scale, individual ‘channel elements,’ which are not always convincingly imaged.

246 Our mapping in the Late Cretaceous Campos basin provide new insights into the
247 depositional products of increased terrigenous sediment supply to the basin margin. The Campos
248 example is particularly impressive because it evolved in a salt-tectonic province. That is, it is
249 impressive that the Campos example exhibits such large meander wavelengths and so much
250 migration because it is surrounded by potentially confining salt diapirs. We speculate that the
251 channel might meander even more, in particular, it might have expanded, or ‘swung’ *sensu* Peakall
252 et al. (2000), to the north and south, if not for confinement from salt-influenced topographic highs.

253 Deep-sea drilling into submarine canyon-fan systems has focused on some of the largest
254 sediment-routing systems in the world (e.g., Deep-Sea Drilling Project Leg 96 of Mississippi Fan,
255 Ocean Drilling Program Leg 155 of Amazon Fan, International Ocean Discovery Program
256 Expedition 354 of Bengal Fans; Bouma et al., 1986; Flood et al., 1995; France-Lanord et al., 2016),
257 with some exceptions (e.g., Ocean Drilling Program Leg 167 of the California margin,
258 International Ocean Discovery Program Expedition 308 of the Brazos-Trinity deep-water
259 depositional system; Piper and Normark, 2001; Pirmez et al., 2012). However, smaller rivers
260 draining rapidly uplifting landscapes can also deliver significant sediment loads to continental
261 margins, promote increased sediment discharge, and form large meandering submarine-channel
262 systems, such as the Late Cretaceous Campos basin fill. These channel systems can disperse
263 terrigenous mass across large areas of continental margins and promote the formation of thick
264 depositional successions recording signals of upstream tectono-climatic perturbations (e.g.,
265 Romans et al., 2016). Studies of these types of deep-water systems linked to small, mountainous
266 rivers can potentially improve understanding of Earth history and the depositional response of
267 continental margins to environmental perturbations.

268 The idea that sediment supply, and not simply drainage area, is the key control on the scale
269 of submarine-channel meanders is useful in predicting large channels in the subsurface of basin
270 margins. For example, in frontier, petroliferous sedimentary basins, thermochronology data can
271 provide clues to the uplift of coastal mountains, which promotes sediment generation and supply
272 to offshore basin-margin canyon-channel-fan systems. Based on our study in the Campos basin,
273 these are the ingredients for the generation of large meandering submarine-channel systems. As a
274 case in point, in the western Gulf of Mexico, a currently active exploration target, Cenozoic uplift
275 of the North American Cordillera, and accelerated uplift of southern Mexico during the late

276 Miocene (Witt et al., 2012; Molina-Garza et al., 2015), promoted the development of the long run-
277 out Veracruz submarine canyon-channel-fan system (Hessler et al., 2018). The presence of this
278 deep-water depositional system was only recently predicted based on provenance analysis of deep-
279 sea drilling (Hessler et al., 2018) coupled with knowledge of the rapid uplift of the sediment source
280 area in southern Mexico. However, subsequent seismic-reflection interpretations in the western
281 Gulf of Mexico revealed meandering submarine-channel systems similar in scale to the Late
282 Cretaceous of the Campos basin (Winter et al., 2017; Clark et al., 2019). Keeping in mind the
283 primary result of our study, that increased sediment supply from small rivers draining uplifting
284 coastal mountain catchments can result in giant meandering submarine-channel systems,
285 knowledge of the sediment source area can be used to predict the scale of meandering submarine-
286 channel systems in a frontier basin.

287

288 **CONCLUSIONS**

289 Some of the largest meandering submarine channels in the world developed in the Campos
290 basin during the Late Cretaceous as a result of increased sediment supply from small, but rapidly
291 uplifting, coastal mountain rivers. Increased sediment discharge promoted the development of
292 these giant meandering submarine channels. The idea that small, mountainous rivers can deliver
293 large sediment discharge to continental margins is not new (Milliman and Syvitski, 1992); we
294 show some of the first detailed imagery and interpretations of the resultant deep-water stratigraphy.
295 Continental margins linked to small, mountainous rivers can contain thick and near-complete
296 accumulations of stratigraphic information of Earth history; moreover, explorers of natural
297 resources might expect to find giant submarine-channel systems in these settings.

298

299 **ACKNOWLEDGMENTS**

300 We thank Investigação Petrolífera Limitada (PGS) for access to seismic-reflection data. We are
301 grateful to Emerson for the access to Paradigm SeisEarth® interpretation and visualization
302 software. We thank the sponsors of the Quantitative Clastics Laboratory (QCL)
303 (<http://www.beg.utexas.edu/qcl>) and the Applied Geodynamics Laboratory (AGL)
304 (<http://www.beg.utexas.edu/agl>). We are grateful to former UT-Austin MS student Can Ceyhan
305 and AGL Principal Investigator Mike Hudec, who initiated collaborative QCL-AGL work on the
306 seismic stratigraphy of the submarine channels in the Campos basin. Gillian Apps and Frank Peel
307 of the AGL also provided valuable insights into submarine channels in the Campos basin.

308

309 **REFERENCES CITED**

- 310 Abreu, V., Sullivan, M., Pirmez, C., and Mohrig, D., 2003, Lateral accretion packages (LAPs); an
311 important reservoir element in deep water sinuous channels: *Marine and Petroleum*
312 *Geology*, v. 20, p. 631-648.
- 313 Azpiroz-Zabala, M., Cartigny, M. J., Talling, P. J., Parsons, D. R., Sumner, E. J., Clare, M. A., ...
314 and Pope, E. L., 2017, Newly recognized turbidity current structure can explain prolonged
315 flushing of submarine canyons: *Science Advances*, v. 3, e1700200.
- 316 Barnes, N. E., and Normark, W. R., 1985, Diagnostic parameters for comparing modern submarine
317 fans and ancient turbidite systems, in Bouma, A.H., Normark, W.R., and Barnes, N.E.,
318 eds., *Submarine fans and related turbidite systems*: New York, NY, Springer, p. 13-14.
- 319 Bouma, A. H., Coleman, J. M., Meyer, A. W., et al., 1986, *Init. Repts. DSDP, 96*: Washington
320 (U.S. Govt. Printing Office).

321 Braun, J., Robert, X., and Simon-Labric, T., 2013, Eroding dynamic topography: Geophysical
322 Research Letters, v. 40, p. 1494-1499.

323 Bruhn, C. H., 1998, Major types of deep-water reservoirs from the eastern Brazilian rift and passive
324 margin basins: AAPG Bulletin, v. 82, p. 1896-1897.

325 Bruhn, C. H., Gomes, J. A. T., Del Lucchese Jr, C., and Johann, P. R., 2003, Campos basin;
326 reservoir characterization and management-Historical overview and future challenges:
327 Offshore Technology Conference.

328 Bruhn, C. H., and Walker, R. G., 1995, High-resolution stratigraphy and sedimentary evolution of
329 coarse-grained canyon-filling turbidites from the Upper Cretaceous transgressive
330 megasequence, Campos Basin, offshore Brazil: Journal of Sedimentary Research, v. 65, p.
331 426-442.

332 Ceyhan, C., 2017, Interplay of salt-influenced structural deformation and submarine channel
333 evolution in the Campos Basin, offshore Brazil [MS Thesis]: The University of Texas at
334 Austin.

335 Clark, J., Ochoa, J., Stockli, D., Fildani, A., Gerber, T., Covault, J., Guzman, J., Vinnels, J., and
336 Marshall, J., 2019, Provenance and Morphology of Extensive Oligocene-Miocene Deep-
337 Water Fan Systems Sourced from Chiapas-Veracruz and Sierra Madre Oriental, Gulf of
338 Mexico: AAPG Annual Convention and Exhibition, San Antonio, Texas, 19-22 May.

339 Cobbold, P. R., Meisling, K. E., and Mount, V. S., 2001, Reactivation of an obliquely rifted
340 margin, Campos and Santos basins, southeastern Brazil: AAPG Bulletin, v. 85, p. 1925-
341 1944.

342 Covault, J. A., Sylvester, Z., Hubbard, S. M., Jobe, Z. R., and Sech, R. P., 2016, The stratigraphic
343 record of submarine-channel evolution: The Sedimentary Record, v. 14, p. 4-11.

344 Covault, J., Sylvester, Z., Hudec, M., Ceyhan, C., and Dunlap, D., 2019, Submarine channels
345 'swept' downstream after bend cutoff in salt basins: The Depositional Record.

346 Davison, I., 2007, Geology and tectonics of the South Atlantic Brazilian salt basins: Geological
347 Society, London, Special Publications, v. 272, p. 345-359.

348 Davison, I., Anderson, L., and Nuttall, P., 2012, Salt deposition, loading and gravity drainage in
349 the Campos and Santos salt basins: Geological Society, London, Special Publications, v.
350 363, p. 159-174.

351 De Gasperi, A., and Catuneanu, O., 2014, Sequence stratigraphy of the Eocene turbidite reservoirs
352 in Albacora field, Campos Basin, offshore Brazil: AAPG Bulletin, v. 98, p. 279-313.

353 Demercian, S., Szatmari, P., and Cobbold, P. R., 1993, Style and pattern of salt diapirs due to thin-
354 skinned gravitational gliding, Campos and Santos basins, offshore Brazil: Tectonophysics,
355 v. 228, p. 393-433.

356 Deptuck, M. E., Steffens, G. S., Barton, M., and Pirmez, C., 2003, Architecture and evolution of
357 upper fan channel-belts on the Niger Delta slope and in the Arabian Sea: Marine and
358 Petroleum Geology, v. 20, p. 649-676.

359 De Ruig, M. J., and Hubbard, S. M., 2006, Seismic facies and reservoir characteristics of a deep-
360 marine channel belt in the Molasse foreland basin, Puchkirchen Formation, Austria: AAPG
361 Bulletin, v. 90, p. 735-752.

362 Eggenhuisen, J. T., and McCaffrey, W. D., 2012, The vertical turbulence structure of experimental
363 turbidity currents encountering basal obstructions; implications for vertical suspended
364 sediment distribution in non-equilibrium currents: Sedimentology, v. 59, p. 1101-1120.

365 Ferry, J. N., Mulder, T., Parize, O., and Raillard, S., 2005, Concept of equilibrium profile in deep-
366 water turbidite system: effects of local physiographic changes on the nature of sedimentary

367 process and the geometries of deposits: Geological Society, London, Special Publications,
368 v. 244, p. 181-193.

369 Fetter, M., 2009, The role of basement tectonic reactivation on the structural evolution of Campos
370 Basin, offshore Brazil; Evidence from 3D seismic analysis and section restoration: *Marine*
371 *and Petroleum Geology*, v. 26, p. 873-886.

372 Fetter, M., De Ros, L. F., and Bruhn, C. H., 2009, Petrographic and seismic evidence for the
373 depositional setting of giant turbidite reservoirs and the paleogeographic evolution of
374 Campos Basin, offshore Brazil: *Marine and Petroleum Geology*, v. 26, p. 824-853.

375 Fildani, A., Hubbard, S. M., Covault, J. A., Maier, K. L., Romans, B. W., Traer, M., and Rowland,
376 J. C., 2013, Erosion at inception of deep-sea channels: *Marine and Petroleum Geology*, v.
377 41, p. 48-61.

378 Flood, R. D., and Damuth, J. E., 1987, Quantitative characteristics of sinuous distributary channels
379 on the Amazon deep-sea fan: *GSA Bulletin*, v. 98, p. 728-738.

380 Flood, R. D., Piper, D. J. W., Klaus, A., et al., 1995, *Proc. ODP, Init. Repts., 155*: College Station,
381 TX (Ocean Drilling Program).

382 France-Lanord, C., Spiess, V., Klaus, A., Schwenk, T., and the Expedition 354 Scientists, 2016,
383 Bengal Fan. *Proceedings of the International Ocean Discovery Program, 354*: College
384 Station, TX (International Ocean Discovery Program).

385 Guardado, L.R., Gamboa, L.A.P. and Lucchesi, C.F., 1989, Petroleum geology of the Campos
386 Basin, Brazil, a model for a producing Atlantic type basin: *AAPG Memoir*, v. 48, p. 3-36.

387 Hessler, A. M., Covault, J. A., Stockli, D. F., and Fildani, A., 2019, Cenozoic cooling favored
388 glacial over tectonic controls on sediment supply to the western Gulf of Mexico: *Geology*,
389 v. 46, p. 995-998.

390 Hodgson, D. M., Di Celma, C. N., Brunt, R. L., and Flint, S. S., 2011, Submarine slope degradation
391 and aggradation and the stratigraphic evolution of channel–levee systems: *Journal of the*
392 *Geological Society*, v. 168, p. 625-628.

393 Howard, A. D., and Hemberger, A. T., 1991, Multivariate characterization of meandering:
394 *Geomorphology*, v. 4, p. 161-186.

395 Hubbard, S. M., Covault, J. A., Fildani, A., and Romans, B. W., 2014, Sediment transfer and
396 deposition in slope channels; deciphering the record of enigmatic deep-sea processes from
397 outcrop: *GSA Bulletin*, v. 126, p. 857-871.

398 Islam, M. R., Begum, S. F., Yamaguchi, Y., and Ogawa, K., 1999, The Ganges and Brahmaputra
399 rivers in Bangladesh; basin denudation and sedimentation: *Hydrological Processes*, v. 13,
400 p. 2907-2923.

401 Karner, G. D., and Gambôa, L. A. P., 2007, Timing and origin of the South Atlantic pre-salt sag
402 basins and their capping evaporites: *Geological Society, London, Special Publications*, v.
403 285, p. 15-35.

404 Kolla, V., Bandyopadhyay, A., Gupta, P., Mukherjee, B., and Ramana, D. V., 2012, Morphology
405 and internal structure of a recent upper Bengal fan-valley complex: *SEPM, Special*
406 *Publications*, v. 99, p. 347-369.

407 Konsoer, K., Zinger, J., and Parker, G., 2013, Bankfull hydraulic geometry of submarine channels
408 created by turbidity currents; Relations between bankfull channel characteristics and
409 formative flow discharge: *Journal of Geophysical Research, Earth Surface*, v. 118, p. 216-
410 228.

411 Kramer, K., Bjerstedt, T. W., and Shedd, W. W., 2016, 3D visualization and characterization of a
412 Mississippi River-scale deepwater channel-levee system on the basin plain, Gulf of
413 Mexico: GCAGS Explore & Discovery Article #0074.

414 Kuhlemann, J., 2007, Paleogeographic and paleotopographic evolution of the Swiss and Eastern
415 Alps since the Oligocene: *Global and Planetary Change*, v. 58, p. 224-236.

416 Leopold, L. B., and Maddock, T., 1953, The hydraulic geometry of stream channels and some
417 physiographic implications: USGS Professional Paper, v. 252, 57 p.

418 Leopold, L. B., and Wolman, M. G., 1960, River meanders: *GSA Bulletin*, v. 71, p. 769-793.

419 Lewis, K. B., 1994, The 1500-km-long Hikurangi Channel; trench-axis channel that escapes its
420 trench, crosses a plateau, and feeds a fan drift: *Geo-Marine Letters*, v. 14, p. 19-28.

421 Luchi, R., Balachandar, S., Seminara, G., and Parker, G., 2018, Turbidity currents with equilibrium
422 basal driving layers; A mechanism for long runout: *Geophysical Research Letters*, v. 45,
423 p. 1518-1526.

424 Macgregor, D. S., 2013, Late Cretaceous–Cenozoic sediment and turbidite reservoir supply to
425 South Atlantic margins: Geological Society, London, Special Publications, v. 369, p. 109-
426 128.

427 Mayall, M., Jones, E., and Casey, M., 2006, Turbidite channel reservoirs—Key elements in facies
428 prediction and effective development: *Marine and Petroleum Geology*, v. 23, p. 821-841.

429 McHargue, T., Pyrcz, M. J., Sullivan, M. D., Clark, J. D., Fildani, A., Romans, B. W., ... and
430 Drinkwater, N. J., 2011, Architecture of turbidite channel systems on the continental slope:
431 patterns and predictions: *Marine and Petroleum Geology*, v. 28, p. 728-743.

432 Meisling, K. E., Cobbold, P. R., and Mount, V. S., 2001, Segmentation of an obliquely rifted
433 margin, Campos and Santos basins, southeastern Brazil: AAPG Bulletin, v. 85, p. 1903-
434 1924.

435 Milani, E. J., Rangel, H. D., Bueno, G. V., Stica, J. M., Winter, W. R., Caixeta, J. M., and Neto,
436 O. P., 2007, Bacias sedimentares brasileiras: cartas estratigráficas: Anexo ao Boletim de
437 Geociências da Petrobrás, v. 15, p. 183-205.

438 Milliman, J. D., and Farnsworth, K. L., 2011, River discharge to the coastal ocean; a global
439 synthesis: Cambridge, UK, Cambridge University Press, 384 p.

440 Milliman, J. D., and Syvitski, J. P., 1992, Geomorphic/tectonic control of sediment discharge to
441 the ocean; the importance of small mountainous rivers: The Journal of Geology, v. 100, p.
442 525-544.

443 Mohriak, W. U., Mello, M. R., Dewey, J. F., and Maxwell, J. R., 1990, Petroleum geology of the
444 Campos Basin, offshore Brazil: Geological Society, London, Special Publications, v. 50,
445 p. 119-141.

446 Mohriak, W., Szatmari, P., and Anjos, S. M. C., 2009, Sal; Geologia e Tectônica: São Paulo,
447 Brazil, Editora Beca, 450 p.

448 Mohriak, W. U., Szatmari, P., and Anjos, S., 2012, Salt; geology and tectonics of selected Brazilian
449 basins in their global context: Geological Society, London, Special Publications, v. 363, p.
450 131-158.

451 Molina-Garza, R. S., Geissman, J. W., Wawrzyniec, T. F., Pena Alonsa, T. A., Iriando, A., Weber,
452 B., and Aranda-Gomez, J., 2015, Geology of the coastal Chiapas (Mexico) Miocene
453 plutons and the Tonalá shear zone; Syntectonic emplacement and rapid exhumation during
454 sinistral transpression: Lithosphere, v. 7, p. 257-274.

455 Mutti, E., and Normark, W. R., 1987, Comparing examples of modern and ancient turbidite
456 systems; problems and concepts, in Leggett J.K., and Zuffa G.G., eds., *Marine Clastic*
457 *Sedimentology*: Dordrecht, Springer, p. 1-38.

458 Normark, W. R., Posamentier, H., and Mutti, E., 1993, Turbidite systems; state of the art and future
459 directions: *Reviews of Geophysics*, v. 31, p. 91-116.

460 Peakall, J., McCaffrey, B., and Kneller, B., 2000, A process model for the evolution, morphology,
461 and architecture of sinuous submarine channels: *Journal of Sedimentary Research*, v. 70,
462 p. 434-448.

463 Peres, W. E. (1993). Shelf-fed turbidite system model and its application to the Oligocene deposits
464 of the Campos Basin, Brazil. *AAPG Bulletin*, 77(1), 81-101.

465 Piper, D. J. W., and Normark, W. R., 2001, Sandy fans-from Amazon to Hueneme and beyond:
466 *AAPG Bulletin*, v. 85, p. 1407-1438.

467 Pirmez, C., 1994, Growth of a submarine meandering channel-levee system on the Amazon Fan
468 [Ph.D. dissertation]: Columbia University.

469 Pirmez, C., and Imran, J., 2003, Reconstruction of turbidity currents in Amazon Channel: *Marine*
470 *and Petroleum Geology*, v. 20, p. 823-849.

471 Pirmez, C., Prather, B. E., Mallarino, G., O'hayer, W. W., Droxler, A. W., Winker, C. D., ... and
472 Mohrig, D., 2012, Chronostratigraphy of the Brazos-Trinity depositional system, western
473 Gulf of Mexico; Implications for deepwater depositional models: *SEPM, Special*
474 *Publications*, v. 99, p. 111-143.

475 Posamentier, H. W., 2003, Depositional elements associated with a basin floor channel-levee
476 system; case study from the Gulf of Mexico: *Marine and Petroleum Geology*, v. 20, p. 677-
477 690.

478 Quirk, D. G., Hertle, M., Jeppesen, J. W., Raven, M., Mohriak, W. U., Kann, D. J., ... and Mendes,
479 M. P., 2013, Rifting, subsidence and continental break-up above a mantle plume in the
480 central South Atlantic: Geological Society, London, Special Publications, v. 369, p. 185-
481 214.

482 Quirk, D. G., Schødt, N., Lassen, B., Ings, S. J., Hsu, D., Hirsch, K. K., and Von Nicolai, C., 2012,
483 Salt tectonics on passive margins; examples from Santos, Campos and Kwanza basins:
484 Geological Society, London, Special Publications, v. 363, p. 207-244.

485 Rangel, H. D., Santos, P. R., and Quintaes, C. M. S. P., 1998, Roncador field, a new giant in
486 Campos basin, Brazil: Offshore Technology Conference.

487 Romans, B. W., Castellort, S., Covault, J. A., Fildani, A., and Walsh, J. P., 2016, Environmental
488 signal propagation in sedimentary timescales systems across: Earth-Science Reviews, v.
489 153, p. 7-29.

490 Schwenk, T., and Spieß, V., 2009, Architecture and stratigraphy of the Bengal Fan as response to
491 tectonic and climate revealed from high-resolution seismic data. SEPM, Special
492 Publications, v. 92, p. 107-131.

493 Sequeiros, O. E., Spinewine, B., Beaubouef, R. T., Sun, T., García, M. H., and Parker, G., 2010,
494 Characteristics of velocity and excess density profiles of saline underflows and turbidity
495 currents flowing over a mobile bed: Journal of Hydraulic Engineering, v. 136, p. 412-433.

496 Sharman, G. R., Hubbard, S. M., Covault, J. A., Hirsch, R., Linzer, H. G., and Graham, S. A.,
497 2018, Sediment routing evolution in the North Alpine Foreland Basin, Austria; interplay
498 of transverse and longitudinal sediment dispersal: Basin Research, v. 30, p. 426-447.

499 Shumaker, L. E., Jobe, Z. R., Johnstone, S. A., Pettinga, L. A., Cai, D., and Moody, J. D., 2018,
500 Controls on submarine channel-modifying processes identified through morphometric
501 scaling relationships: *Geosphere*, v. 14, p. 2171-2187.

502 Summerfield, M. A., and Hulton, N. J., 1994, Natural controls of fluvial denudation rates in major
503 world drainage basins: *Journal of Geophysical Research, Solid Earth*, v. 99, p. 13871-
504 13883.

505 Sylvester, Z., and Covault, J. A., 2016, Development of cutoff-related knickpoints during early
506 evolution of submarine channels: *Geology*, v. 44, p. 835-838.

507 Sylvester, Z., Durkin, P., and Covault, J. A., 2019, High curvatures drive river meandering:
508 *Geology*, v. 47, p. 263-266.

509 Sylvester, Z., Pirmez, C., and Cantelli, A., 2011, A model of submarine channel-levee evolution
510 based on channel trajectories; Implications for stratigraphic architecture: *Marine and*
511 *Petroleum Geology*, v. 28, p. 716-727.

512 Sylvester, Z., Pirmez, C., Cantelli, A., and Jobe, Z. R., 2013, Global (latitudinal) variation in
513 submarine channel sinuosity; Comment: *Geology*, v. 41, p. e287-e287.

514 Sylvester, Z., and Pirmez, C., 2017, Latitudinal Changes in the Morphology of Submarine
515 Channels; Reevaluating the Evidence for the Influence of the Coriolis Force. *SEPM,*
516 *Special Publications*, v. 108.

517 Thompson, R. N., Gibson, S. A., Mitchell, J. G., Dickin, A. P., Leonardos, O. H., Brod, J. A., and
518 Greenwood, J. C., 1998, Migrating Cretaceous–Eocene Magmatism in the Serra do Mar
519 Alkaline Province, SE Brazil; Melts from the Deflected Trindade Mantle Plume?: *Journal*
520 *of Petrology*, v. 39, p. 1493-1526.

521 Williams, G. P., 1986, River meanders and channel size: *Journal of hydrology*, v. 88, p. 147-164.

522 Winter, R., Dailey, D., Wigger, S., Heyn, T., Jaminski, J., Beaman, M., and O'Leary, J., 2017,
523 Complex Sediment Dispersal in the Campeche Deepwater Province, Offshore Southern
524 Mexico—An Example of a Hybrid Tectonically Active Margin: AAPG Annual Convention
525 and Exhibition, Houston, Texas, 2-5 April.

526 Winter, W. R., Jahnert, R. J., and França, A. B., 2007, Bacia de campos: Boletim de Geociencias
527 da Petrobras, v. 15, p. 511-529.

528 Witt, C., Brichau, S., and Carter, A., 2012, New constraints on the origin of the Sierra Madre de
529 Chiapas (south Mexico) from sediment provenance and apatite thermochronology:
530 Tectonics, v. 31, p. 1-15.

531 Wolman, M. G., and Miller, J. P., 1960, Magnitude and frequency of forces in geomorphic
532 processes: The Journal of Geology, v. 68, p. 54-74.

533

534 **FIGURE CAPTIONS**

535 Figure 1. Study area in the deep-water Campos Basin. Gray polygon indicates location of seismic-
536 reflection volume and maps in Figures 3 and 5. Modified from Peres (1993).

537 Figure 2. Structure maps of horizons bounding the Late Cretaceous channel system in the Campos
538 basin. Black lines indicate locations of cross sections in Figure 3.

539 Figure 3. Cross sections of the Campos basin channel system between horizons 1 and 3. Black
540 dashed rectangles in seismic-reflection profiles A-A' and B-B' indicate locations of
541 depositional elements in line-drawing interpretations. In cross section A-A', overlying
542 Horizon 3, discontinuous, high-amplitude seismic reflections are Cenozoic channel
543 deposits, including the Miocene channel system of Covault et al. (2019).

544 Figure 4. Concept of bankfull depth of a meandering channel system as a basis for measuring
545 channel geometry. (A) Seafloor of the Bengal channel. Note the relatively narrow, sinuous
546 channel form in the deepest location in the valley (i.e., the thalweg). Modified from Kolla
547 et al. (2012). Map (B) and cross-section (C) views of a forward model of a submarine
548 channel-levee system from Sylvester and Covault (2016) and Covault et al. (2016).

549 Figure 5. (A) RMS amplitude map between horizons 1 and 2. (B) Interpretation of channel forms.
550 (C) RMS amplitude map between horizons 2 and 3. (D) Interpretation of last channel form
551 in the system.

552 Figure 6. Submarine and fluvial channel wavelength vs. width. See ‘How do we measure the size
553 of a submarine channel?’ for methods of measurement (Sylvester et al., 2013; Sylvester
554 and Pirmez, 2017). Black boxes indicate measurements of channels in the Campos basin.
555 Lower right, inset: Campos channel bends we felt most confident in measuring in the
556 seismic-reflection data.

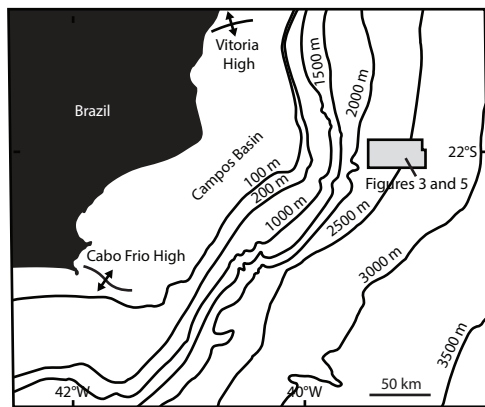


Figure 1.

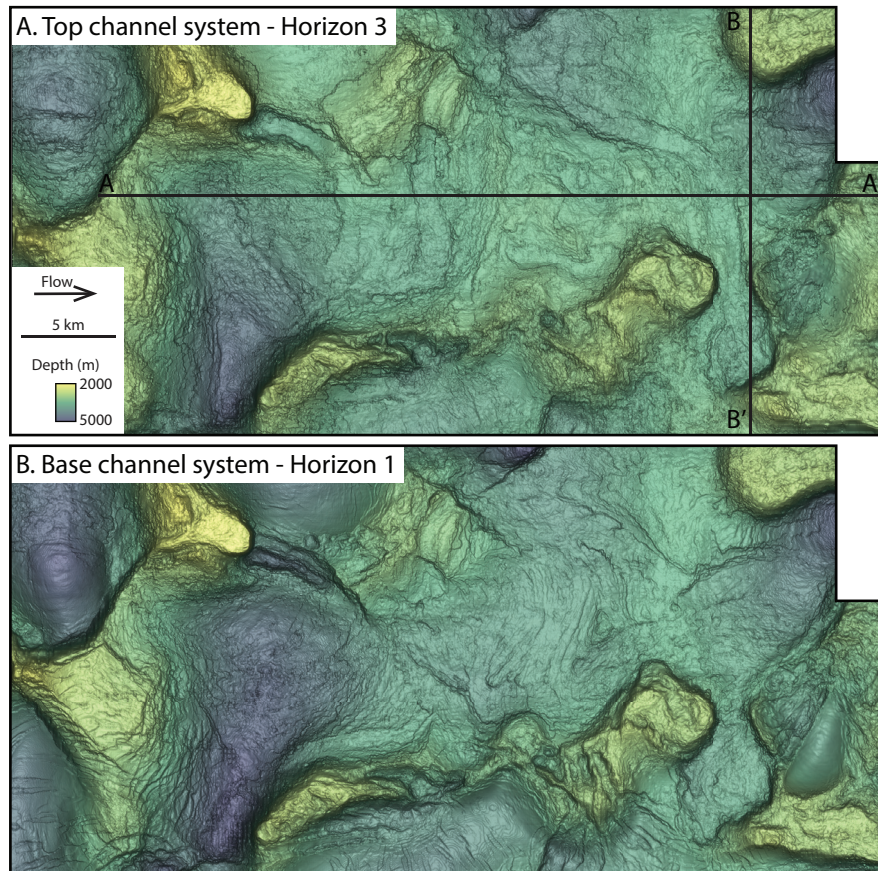


Figure 2.

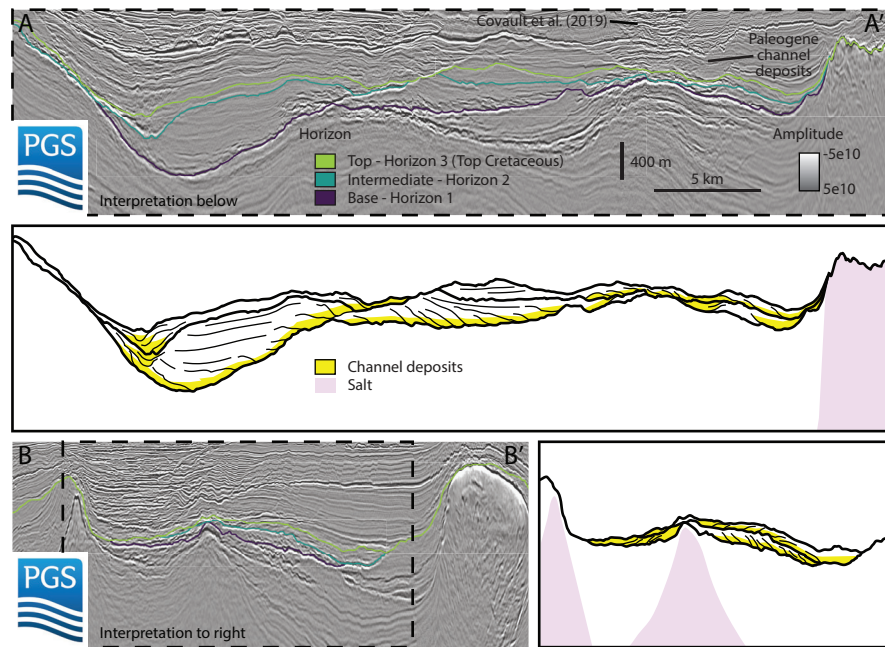


Figure 3.

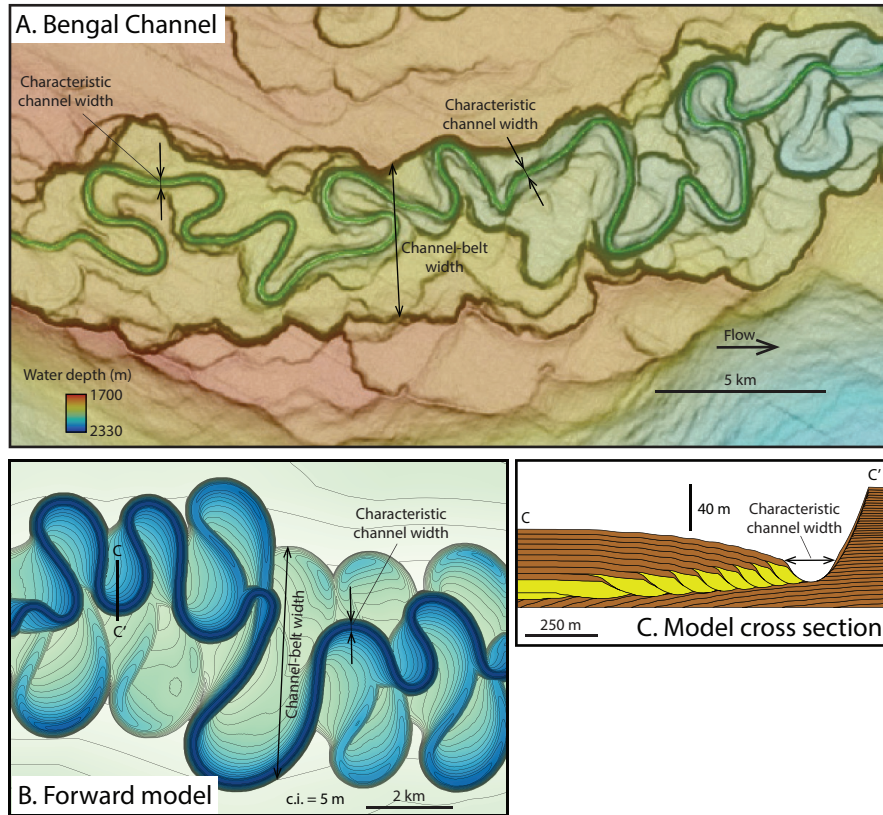


Figure 4.

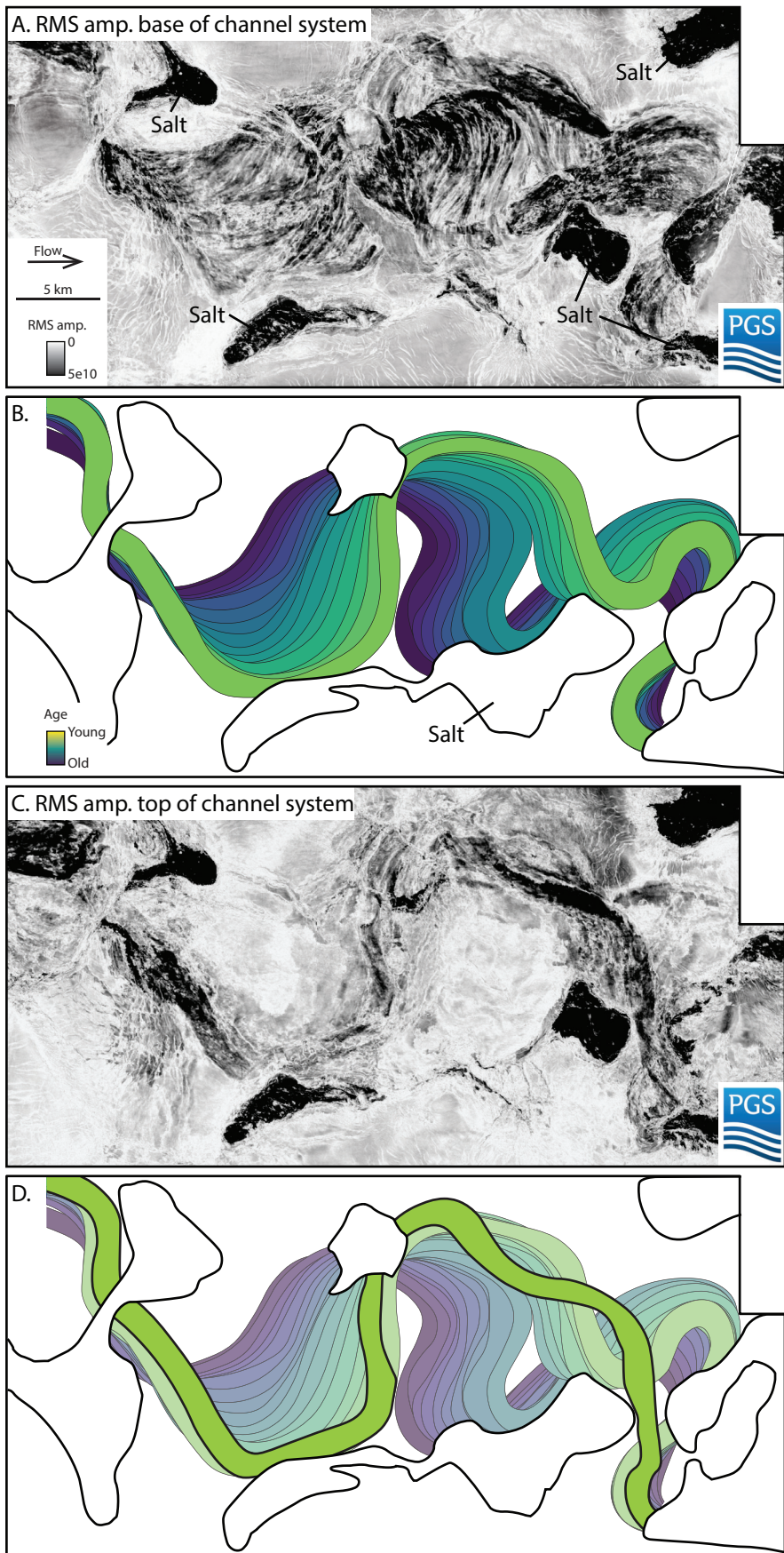


Figure 5.

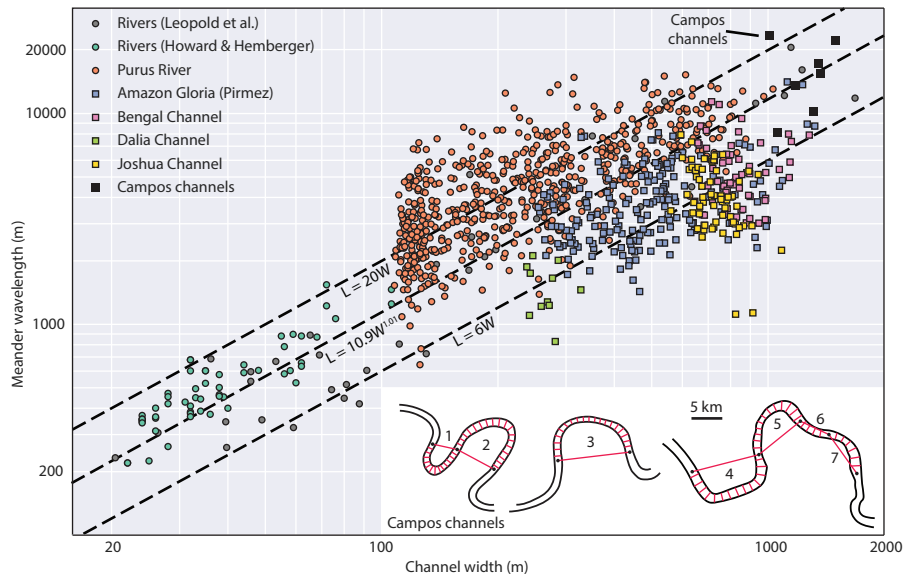


Figure 6.